ILL Number: 15333058

RAPID

MIT Libraries Document Services/Interlibrary Loan

ILLiad TN: 605940

Delivery Method: Odyssey

Borrower: RAPID:GZM

Request Date: 10/25/2019 8:49:04 AM

Call #: QC.R129

Lending String:

Location: Isa 4

Journal Title: Radiology

Vol.: 219 Issue: 2
Month/Year: 2001
Pages: 535-540

Notes:

Author: Groenink, M.

Title: Biophysical properties of the normal-sized aorta in patients with Marfan syndrome: evaluation with MR flow mapping

Imprint:

OCLC#: 94197

Billing Exempt

Patron:

Odyssey: madison.hosts.atlas-sys.com

Ariel: 128.104.61.85

Email Address:

US Copyright Notice

The copyright law of the United States (Title 17, United States Code) governs the making of reproductions of copyrighted material. Under certain conditions specified in the law, libraries are authorized to furnish a reproduction. One of these specified conditions is that the reproduction is not to be "used for any purpose other than private study, scholarship, or research." If a user makes a request for, or later uses, a reproduction for purposes in excess of "fair use," that user may be liable for copyright infringement. This institution reserves the right to refuse to accept a copying order if, in its judgment, fulfillment of the order would involve violation of Copyright Law.

Maarten Groenink, MD
Albert de Roos, MD
Barbara J. M. Mulder, MD
Ben Verbeeten, Jr, MD
Janneke Timmermans, MD
Aeilko H. Zwinderman, PhD
Jos A. E. Spaan, PhD
Ernst E. van der Wall, MD

Index terms:
Aorta, flow dynamics
Aorta, MR, 941.129411, 941.12944, 943.129411, 943.129412, 943.12944
Magnetic resonance (MR), vascular studies, 941.129411, 941.129412, 941.12944, 943.129411, 943.129412, 943.12944
Marfan syndrome, 941.1971, 943.1971

Radiology 2001; 219:535–540

[1] From the Departments of Cardiology (M.G., B.J.M.M.), Radiology (B.V.), and Medical Physics (J.A.E.S.), Academic Medical Center, Amsterdam, the Netherlands; the Departments of Cardiology (M.G., E.E.v.d.W.), Radiology (M.G., A.d.R.), and Biostatistics (A.H.Z.), Leiden University Medical Center, Albinusdreef 2, 2333 AA Leiden, the Netherlands; and the Department of Cardiology, Nijmegen University Hospital, the Netherlands (J.T.). Received June 1, 2000; revision requested July 17; final revision received October 30; accepted November 20. M.G. supported by the Interuniversity Cardiology Institute of the Netherlands and the SORBO Heart Foundation. **Address correspondence to** A.d.R. (e-mail: *a.de_roos@lumc.nl*).

© RSNA, 2001

Author contributions:
Guarantors of integrity of entire study, M.G., A.d.R., B.J.M.M., E.E.v.d.W.; study concepts and design, M.G., A.d.R., B.J.M.M., E.E.v.d.W.; literature research, M.G.; clinical studies, M.G., B.J.M.M., E.E.v.d.W., J.T.; data acquisition, M.G., B.V.; data analysis/interpretation, M.G., B.J.M.M., A.H.Z., J.A.E.S., J.T.; statistical analysis, M.G., A.H.Z.; manuscript preparation and definition of intellectual content, M.G., A.d.R., B.J.M.M., E.E.v.d.W., B.V.; manuscript editing, M.G., A.d.R., B.J.M.M., E.E.v.d.W.; manuscript revision/review and final version approval, all authors.

Biophysical Properties of the Normal-sized Aorta in Patients with Marfan Syndrome: Evaluation with MR Flow Mapping[1]

PURPOSE: To investigate the feasibility of magnetic resonance (MR) flow mapping in the assessment of aortic biophysical properties in patients with Marfan syndrome and to detect differences in biophysical properties in the normal-sized aorta distal to the aortic root between these patients and matched control subjects.

MATERIALS AND METHODS: Seventy-eight patients with Marfan syndrome with aortic root dilatation and 23 matched control subjects underwent MR flow mapping in four locations in the normal-sized aorta (1, ascending aorta; 2, thoracic descending aorta; 3, descending aorta at the level of the diaphragm; and 4, abdominal descending aorta). Distensibility at each location and flow wave velocity between locations were calculated.

RESULTS: Compared with the control subjects, patients with Marfan syndrome had decreased aortic distensibility at three of the four locations (levels 1, 2, and 4; $P < .05$) and increased flow wave velocity between all locations ($P < .05$) in the aorta. In patients with Marfan syndrome, flow wave velocity was also significantly increased along the entire aortic tract beyond the aortic root (from level 1 to level 4).

CONCLUSION: MR imaging reveals abnormal biophysical properties of the normal-sized aorta in patients with Marfan syndrome. Monitoring of these properties is relevant for evaluating disease progression and treatment options.

Marfan syndrome is a heritable disorder of connective tissue resulting in a highly variable degree of premature aortic medial degeneration with a high risk of subsequent dissection or rupture (1–5). Although most mortality due to aortic dissection and rupture has been related to aortic aneurysm size and expansion rate, clear guidelines for surgical intervention remain scarce due to the precarious clinical course of the process of aortic dilation, dissection, and rupture (6–9). Biophysical properties of the aorta may have additional prognostic value regarding the occurrence of aortic dilation, dissection, and rupture in aortic degenerative disease and may contribute to the risk stratification of patients at risk for aortic complications (10,11). Biophysical properties of the aorta can be expressed in terms of distensibility (percentage of luminal increase per pressure increase [in millimeters of mercury] during a heart beat cycle) or the propagation velocity of the pulse or flow wave through the aorta (pulse wave velocity, flow wave velocity) (10–14). Magnetic resonance (MR) imaging has been recommended (15–17) as the technique of first choice for the detection and follow-up of both aortic complications and premorbid conditions, such as intramural hematoma and aortic aneurysm. In addition, assessment of aortic distensibility and flow wave velocity are feasible with MR imaging (18–21).

The purpose of the present study was (*a*) to investigate the feasibility of MR imaging in the assessment of aortic biophysical properties in patients with Marfan syndrome and (*b*) to detect differences in biophysical properties in the aortic tract distal to the aortic root between these patients and matched control subjects.

MATERIALS AND METHODS

The study design was reviewed and approved by local institutional review boards.

Study Subjects

After written informed consent was obtained, 88 consecutive patients with Marfan syndrome (mean age, 31 years; age range, 18–50 years) without a history of aortic dissection, aortic surgery, or aneurysms in the aortic tract distal to the aortic root were initially included and referred for MR imaging from September 1996 to May 1997. Aortic root diameter in all patients was less than 50 mm, and no evident aortic regurgitation was present, as shown at echocardiography. In all patients, Marfan syndrome was definitely diagnosed by one of the multidisciplinary screening teams from four university hospitals according to the revised guidelines by De Paepe et al (22).

In each study subject, length and weight were determined, and body surface area was calculated (23). After the initial inclusion of the 88 patients, 10 (11%) patients were excluded. In the excluded patients, MR imaging revealed a large abdominal aortic aneurysm with thrombus in one patient. In two patients, triggering problems during image acquisition precluded accurate image analysis. In seven patients, MR images could not be properly analyzed because of poor image quality. In five patients, this poor quality was due to artifacts from a steel bar in the vertebral column (Harrington bar correction for severe scoliosis) at some of the defined aortic levels; in two patients, this was due to motion artifacts. Seventy-eight patients with Marfan syndrome (46 men [mean age, 30 years; age range, 18–50 years], 32 women [mean age, 32 years; age range, 20–46 years]) remained for analysis. A total of 23 age- and sex-matched healthy control subjects was considered statistically appropriate for comparison purposes (see Statistical Analysis). This group served as a reference population after written consent was obtained. Study group characteristics are shown in Table 1.

TABLE 1
Study Subject Characteristics

Characteristic	Marfan Syndrome Group (n = 78)	Control Group (n = 23)
Sex*		
Male	46 (59)	9 (39)
Female	32 (41)	14 (61)
Age (y)	31 ± 8	28 ± 6
Body surface area (m^2)	2.01 ± 0.19	1.88 ± 0.18
Mean blood pressure (mm Hg)	80 ± 8	81 ± 10

Note.—For comparisons of all characteristics, P values were greater than .05 except for body surface area (P = .006).
*Data in parentheses are percentages.

MR Imaging

MR imaging was performed with a 1.5-T (ACS-NT15, Philips Medical Systems, Best, the Netherlands; Magnetom Vision, Siemens, Erlangen, Germany) by using similar pulse sequences. Image acquisition was triggered on the electrocardiogram. The entire aorta was imaged in the transverse and oblique sagittal planes by using a standard spin-echo pulse sequence. Next, a gradient-echo pulse sequence with velocity encoding (FLASH2D [Siemens] with a 24-msec repetition time and a 5-msec echo time or FFE [Philips] with a repetition time equal to the RR interval [in milliseconds] and a 14-msec echo time; matrix size, 256 × 256; field of view, 300 mm; section thickness, 8 mm; flip angle, 20°) was applied perpendicular to the aorta at four levels, as indicated in Figure 1: 1, perpendicular to the ascending aorta at the level of the bifurcation of the pulmonary artery; 2, perpendicular to the descending aorta at the level of the bifurcation of the pulmonary artery; 3, at the level of the diaphragm; and 4, just above the aortic bifurcation. Maximal velocity encoding was routinely chosen at 150 cm/sec and was increased to a maximum of 250 cm/sec when aliasing occurred. This pulse sequence generated phase-related pairs of modulus and velocity-encoded images with a temporal resolution of approximately 25 msec and a spatial resolution of 1 pixel/mm in the x-y direction.

The length of the three segments encompassed by the four levels were measured by drawing a line through the middle of the aortic lumen from each level to another on the oblique sagittal images by using the console of the MR system (Fig 1). This was performed by one author (M.G.). An additional flow measurement, with the same pulse sequence, was applied perpendicular to the aortic root at the level of the sinus of Valsalva to rule out aortic regurgitation and to measure diastolic aortic root size. During each flow measurement, the brachial artery systolic and diastolic blood pressures were measured three times by means of a sphygmomanometer cuff. Mean blood pressure (MBP) was calculated from systolic and diastolic blood pressures (SBP and DBP, respectively) by using the following equation: MBP = [(2 × DBP) + SBP]/3. During each flow measurement, heart rate was monitored by means of the electrocardiogram.

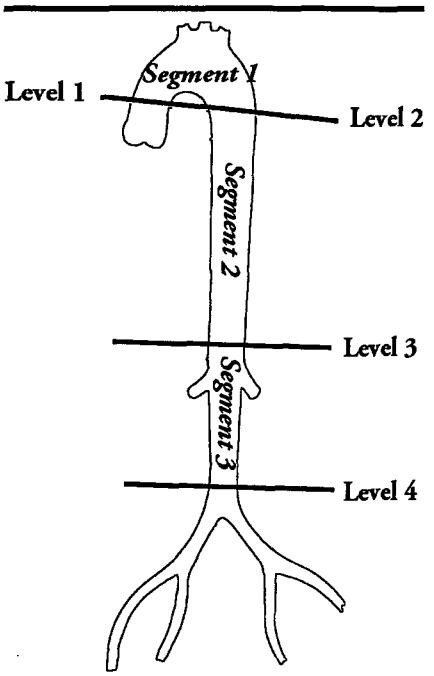

Figure 1. Schematic shows levels perpendicular to the aorta applied for gradient-echo MR imaging with velocity encoding. Distensibility and diastolic aortic diameter were assessed at these four levels, which encompass three aortic segments. Flow wave velocity along each of the three segments was calculated.

Image Analysis and Calculations

A workstation (Sparc Ultra; Sun Microsystems; Mountain View, Calif) and FLOW image analysis software (Medis, Leiden, the Netherlands) were used for image analysis. Aortic contours were drawn manually (by M.G.) on the modulus images of all cardiac phases, and flow (in milliliters per second) through each aortic level was calculated by using the areas on the modulus images and the velocity values of the

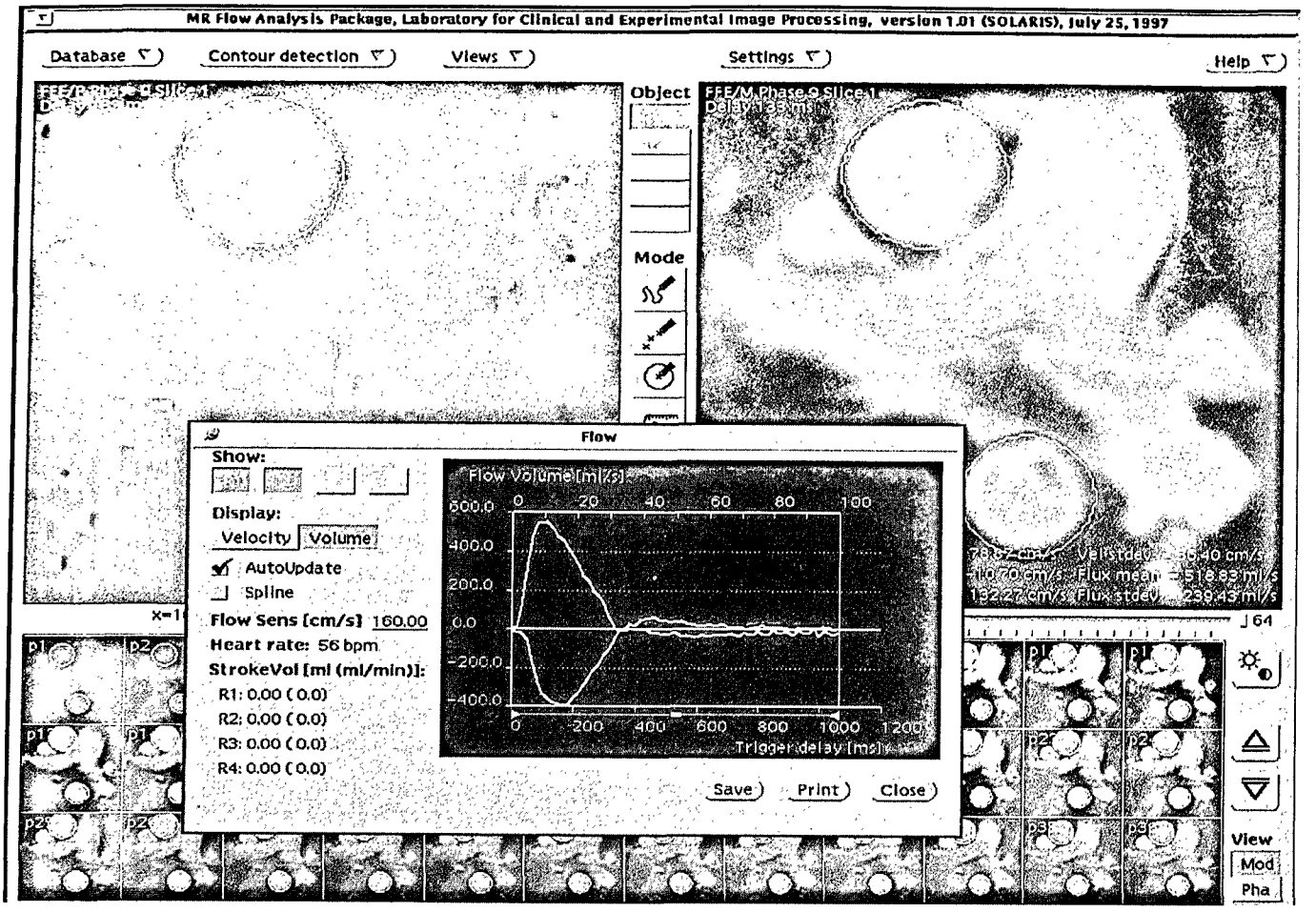

Figure 2. Screen shot shows analysis with the FLOW (Medis) software package. A transverse plane at levels 1 and 2 (through the ascending and descending aorta) is shown. Contours of the ascending (upper circle) and descending (lower circle) aorta are drawn on the module image on the right and encompass the velocity-encoded area on the phase image on the left.

corresponding velocity-encoded images (Fig 2). Flow wave velocity (in meters per second) was calculated as the ratio of the distance between two levels and the time difference between arrival of the flow wave at these levels. The flow wave was considered to arrive at a certain level when the flow reached half of its maximum value (Fig 3). Consequently, flow wave velocity in the entire aorta distal to the aortic root (from level 1 to level 4) and flow wave velocity in three segments of the aorta (ascending aorta–aortic arch, thoracic descending aorta, and abdominal descending aorta) were determined.

Distensibility at the four levels was calculated by means of the following equation: $D = (A_{max} - A_{min}) \div [A_{min} \times (P_{max} - P_{min})]$, where D is distensibility (in millimeters of mercury^{-1}), A_{max} is the maximal (systolic) aortic area (in square millimeters), A_{min} is the minimal (diastolic) aortic area (in square millimeters), P_{max} is the systolic blood pressure (in millimeters of mercury), and P_{min} is the diastolic blood pressure (in millimeters of mercury).

To compare aortic size among groups, the diastolic diameters of the aortic root and those at levels 1–4 were divided by the body surface area to yield body surface area–corrected diameters.

Interobserver Agreement

Interobserver variation in measurement of systolic and diastolic aortic areas, drawn by two independent observers (M.G., B.J.M.M.), was studied in eight control subjects and 15 patients with Marfan syndrome by using 85 measurements at several aortic levels. Interobserver variation of calculated flow wave velocities was assessed in 34 randomly selected segments in eight control subjects and in 51 randomly selected segments in 15 patients with Marfan syndrome.

Statistical Analysis

Results are expressed as the mean plus or minus 1 SD unless otherwise specified. Observer agreement was quantified by using intraclass correlation coefficients (r_{ic}). Group means of the data were analyzed by using the two-sample Student t test. A P value less than .05 was considered to indicate a statistically significant difference. In total, data from 23 healthy control subjects were available for comparison. The sample size of 23 healthy control subjects yielded a power of at least 80% for a 1 m/sec difference in flow wave velocity between patients with Marfan syndrome and healthy control subjects when an SD of 1 m/sec in the healthy control subjects was assumed.

RESULTS

Reproducibility of Measurements

Measurement of the systolic and diastolic aortic areas proved to be reproducible, with a mean difference of 1 mm^2 ± 13 between the two observers (0% ± 3.5 of the mean aortic area, r_{ic} = 0.9984). A

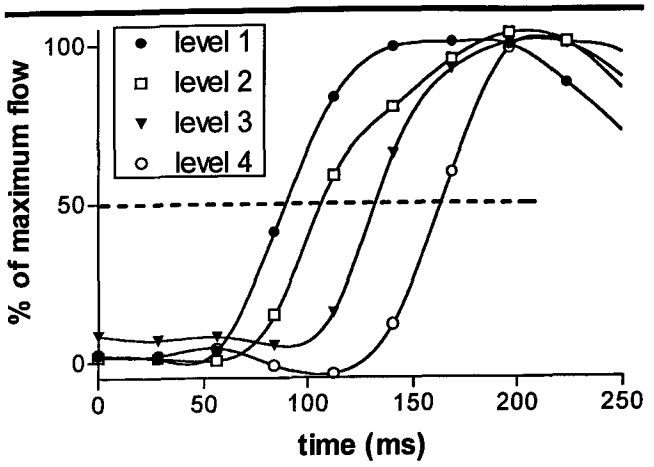

Figure 3. Graph shows a typical example of the propagation of the flow wave along the aorta as a function of time. Assessment of the time lag between arrival of the flow wave between the four levels was achieved by using the point of half-maximum flow (in milliliters per second), as indicated by the dashed line.

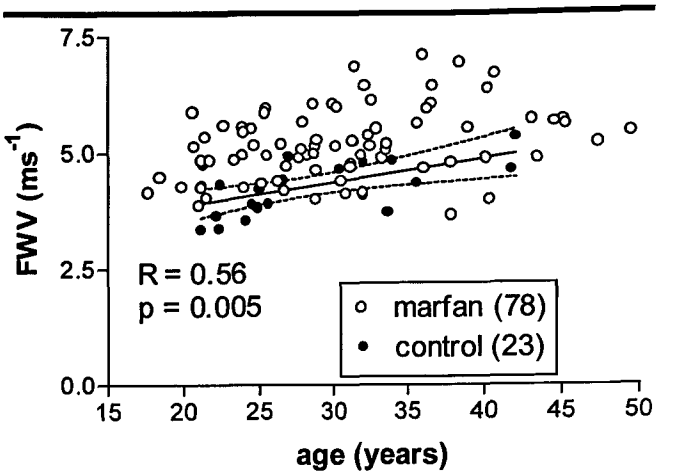

Figure 4. Graph shows the linear correlation between age and flow wave velocity (*FWV*) along the entire aorta in the control subjects (●). The 95% confidence limits of the true regression line are indicated with dashed lines. ○ = data in patients with Marfan syndrome. Numbers in parentheses are the number of subjects in each group.

good interobserver correlation was also shown in flow wave velocities between several levels, with a mean difference of -0.04 msec^{-1} ± 0.3 (-0.4% ± 4 of the mean flow wave velocity, r_{ic} = 0.9984) between the two observers.

Blood Pressure and Heart Rate during MR Imaging

No statistically significant difference in mean blood pressure between patients with Marfan syndrome and control subjects was shown. Blood pressure and heart rate remained relatively constant during the imaging session. In 22 (95%) of the control subjects, variation in mean blood pressure did not exceed 7 mm Hg. In 74 (95%) of the patients with Marfan syndrome, variation in mean blood pressure did not exceed 5 mm Hg. In 22 (95%) of the control subjects and in 74 (95%) patients with Marfan syndrome, heart rate did not vary more than 2 beats per minute during the imaging session.

Aortic Dimensions and Valve Function

Aortic root diameters, normalized for body surface area, were significantly larger in the patients than in the control subjects, confirming the diagnosis of Marfan syndrome. No significant differences in body surface area–corrected diameters at any of the four aortic levels distal to the aortic root were found between patients with Marfan syndrome and control subjects (Table 2). No regurgitant fractions greater than 5% were found in the patients with Marfan syndrome or in the control subjects.

TABLE 2
Dimensions and Biophysical Properties of the Aorta in the Study Subjects

Dimension or Property	Marfan Syndrome Group	Control Group	*P* Value
Aortic root diameter (mm)	43 ± 6	32 ± 3	<.001
Body surface area–indexed diameter (mm/m^2)			
Aortic root	21 ± 3	17 ± 2	<.001
Level 1	15 ± 2	15 ± 2	>.05
Level 2	12 ± 1	11 ± 1	>.05
Level 3	10 ± 1	10 ± 1	>.05
Level 4	9 ± 2	9 ± 1	>0.5
Distensibility (10^{-3} mm Hg^{-1})			
Level 1	3.0 ± 2.6	4.4 ± 2.2	.03
Level 2	3.4 ± 1.9	4.6 ± 1.5	.01
Level 3	5.1 ± 2.0	5.4 ± 2.3	>0.5
Level 4	3.8 ± 2.2	5.2 ± 3.4	.02
Flow wave velocity (msec^{-1})			
Level 1 to level 2	4.4 ± 1.1	3.8 ± 0.7	.01
Level 2 to level 3	6.7 ± 2.2	4.6 ± 0.9	<.001
Level 3 to level 4	5.5 ± 1.5	4.5 ± 0.9	.003
Level 1 to level 4	5.2 ± 0.8	4.3 ± 0.6	<.001

Aortic Elastic Properties

Significant differences in aortic distensibility were shown at levels 1, 2, and 4. Figure 3 shows a typical example of the propagation of the flow wave along the aorta as a function of time. The time differences between arrival of half-maximum flow at the four levels are clearly visible. Significant differences in flow wave velocities between patients with Marfan syndrome and control subjects were shown in all three aortic segments and in the entire aorta distal to the aortic root. Furthermore, we observed a significant correlation between age and entire aortic flow wave velocity in the control subjects (r = 0.56, P = .005) (Fig 4), which was not seen in the patients with Marfan syndrome. Table 2 shows the data regarding aortic elastic properties.

DISCUSSION

In the present study, we used MR imaging techniques to investigate aortic biophysical properties in a large population of patients with relatively uncomplicated Marfan syndrome and in a group of matched control subjects. It was shown that significantly decreased aortic distensibility and increased flow wave velocity can be detected in undilated aortic tracts distal to the aortic root of patients with Marfan syndrome.

Methodologic Considerations

MR imaging techniques appeared to be adequate for the measurement of aortic biophysical properties in the majority of patients with Marfan syndrome.

Because aortic biophysical properties change with increasing pressure due to the recruitment of collagen fibers, distensibility reflects only the mean of aortic elastic behavior in the physiologic pressure range (24). Moreover, noninvasively determined brachial artery systolic and diastolic blood pressures may not be accurate enough to allow calculation of aortic distensibility in vivo (14,25). Distensibility also depends on the degree of diastolic distention (diastolic size), as shown by Jeremy et al (26), who used echocardiography to assess elastic properties of the ascending aorta in patients with Marfan syndrome and in control subjects. In the present study, patients and control subjects did not significantly differ in aortic size; this finding should rule out this effect.

In general, fibrillar fragmentation in the aortic media of patients with Marfan syndrome is scattered in an irregular pattern along the aorta (27). As a result, distensibility may relate to more affected or less affected parts of the aorta, depending on the chosen aortic level. All these factors could explain the large variations in aortic distensibility found in our study and reported in earlier articles (19,21,28–32). Lehmann (11,25) and Lehmann et al (25) have recommended the use of the propagation velocity of the pulse wave to assess aortic biophysical properties because of the greater reproducibility and relative pressure independence of this elastic index. Even the use of this index as a risk factor for a broader range of cardiovascular events has been proposed (11).

The velocity of the pulse wave in the human aorta has previously been measured by Latham et al (33), who used a catheter with micromanometers separated by 5 cm to invasively assess pulse wave velocity. Mean values obtained by Latham et al (aortic arch, 4.4 $msec^{-1}$; thoracic descending aorta, 5.2 $msec^{-1}$; and abdominal descending aorta, 5.7 $msec^{-1}$) are well within the values for flow wave velocities obtained in our study by considering the addition of two SDs to the mean values of the 23 control subjects (5.2, 6.4, and 6.3 $msec^{-1}$, respectively). Our results also agree well with pulse wave velocity (34,35) and MR flow wave velocity (20,36,37) measurements by other investigators. They contrast, however, with values of 8–12 $msec^{-1}$ for pulse wave velocity in the descending aorta obtained by means of carotid and femoral tonometry or Doppler ultrasonography in healthy control subjects and patients (11,28). High pulse wave velocities in the carotid and iliac tracts and unawareness about the actual length of an aortic segment could explain this phenomenon.

Aortic Biophysical Properties in Patients with Marfan Syndrome

Decreased aortic distensibility in patients with Marfan syndrome has been shown in a number of studies (19,21,28–32), with mean values of 2–8 (10^{-3} mm Hg^{-1}) in the ascending aorta, 3–6 (10^{-3} mm Hg^{-1}) in the thoracic descending aorta, and 5–6 (10^{-3} mm Hg^{-1}) in the abdominal aorta. Distensibility values in the present study (Table 2) are in the lower range of these values, which seems surprising in view of the fact that patients with rather uncomplicated Marfan syndrome were examined. On the other hand, in a study by Savolainen et al (30), who used gradient-echo MR imaging to assess distensibility in children with Marfan syndrome (mean age, 11 years), ascending aortic distensibility was nearly twice the mean value in the present study; this finding may be indicative of a rapid decrease in aortic distensibility in the 2nd decade of life.

Hirata et al (29) studied pulse wave velocity along the descending aorta in patients with Marfan syndrome by using carotid and femoral tonometry, and they reported a substantially increased value of 11.6 $msec^{-1}$ in patients with Marfan syndrome. In the control group described by Hirata et al, the mean pulse wave velocity was 9.5 $msec^{-1}$, which still seems excessively high compared with our data. Although age correlated with flow wave velocity in the control group, this phenomenon was not observed in the Marfan syndrome group. This finding is probably due to extreme variation in the extent of medial degeneration that outweighed the effects of aging within the narrow age boundaries of our study population.

In conclusion, MR imaging enables the assessment of aortic biophysical properties in patients with Marfan syndrome. Although some overlap in values for biophysical properties between patients with Marfan syndrome and matched control subjects is apparently present, we conclude that by using this technique, significantly increased flow wave velocity and decreased distensibility can be detected in patients with Marfan syndrome without dilatation in the aortic tract distal to the aortic root. This finding could be of clinical use in the identification of patients who are especially at risk for aortic dilatation and dissection before the aorta is dilated. Further studies, however, are required to assess the predictive value of biophysical properties on the occurrence of aortic complications.

References

1. Dietz HC, Cutting GR, Pyeritz RE, et al. Marfan syndrome caused by a recurrent de novo missense mutation in the fibrillin gene. Nature 1991; 352:227–339.
2. Murdoch JL, Walker BA, Halpern BL, Kuzma JW, McKusick VA. Life expectancy and causes of death in the Marfan syndrome. N Engl J Med 1972; 286:804–808.
3. Silverman DI, Burton KJ, Gray JJ, et al. Life expectancy in the Marfan syndrome. Am J Cardiol 1995; 75:157–160.
4. Gott VL, Pyeritz RE, Cameron DE, et al. Composite graft repair of Marfan aneurysms of the ascending aorta: results in 100 patients. Ann Thorac Surg 1991; 52: 38–44.
5. Pyeritz RE. Disorders of fibrillins and microfibrilogenesis: Marfan syndrome, MASS phenotype, contractural arachnodactyly and related conditions. In: Emery AE, Rimoin DL, David L, Connor JM, Pyeritz RE, eds. Principles and practice of medical genetics. 3rd ed. New York, NY: Churchill Livingstone, 1996.
6. Gott VL, Greene PS, Alejo DE, Cameron DE, Naftel DC, Miller DC. Replacement of the aortic root in patients with Marfan's syndrome. N Engl J Med 1999; 340:307–313.
7. Pitt MP. Bonser RS. The natural history of thoracic aortic aneurysm disease: an overview. J Cardiac Surg 1997; 12:270–278.
8. Sütch G, Jenni R, von Segesser L, Turina M. Predictability of aortic dissection as a function of aortic diameter. Eur Heart J 1991; 12:1247–1256.
9. Groenink M, Lohuis TAJ, Tijssen JGP, et al. Survival and complication-free survival in Marfan's syndrome: implications of current guidelines. Heart 1999; 82:499–504.
10. Groenink M, Langerak SE, Vanbavel E, et al. The influence of aging and aortic stiffness on permanent dilation and breaking stress of the thoracic descending aorta. Cardiovasc Res 1999; 43:471–480.
11. Lehmann ED. Clinical value of aortic pulse wave velocity measurement. Lancet 1999; 354:528–529.
12. Stefanadis C, Stratos C, Boudoulas H, Kourouklis C, Toutouzas P. Distensibility of the ascending aorta: a comparison of invasive and non-invasive techniques in healthy men and in men with coronary artery disease. Eur Heart J 1990; 11:990–996.
13. Bramwell JC, Hill AY. Velocity of transmission of the pulse-wave and elasticity of arteries. Lancet 1922; 891–892.
14. Lehmann ED, Gosling RG, Parker JR, de-Silva T, Taylor MG. A blood pressure independent index of aortic distensibility. Br J Radiol 1993; 66:126–131.
15. Nienaber CA, von Kodolitsch Y, Peterson B, Loose R, Helmchen A, Spielmann R. Intramural hemorrhage of the aorta: diagnostic and therapeutic implications. Circulation 1995; 92:1465–1472.
16. Kawamoto S, Bluemke DA, Traill TA, Zerhouni EA. Thoracoabdominal aorta in

Marfan syndrome: MR imaging findings of progression of vasculopathy after surgical repair. Radiology 1997; 203:727–732.
17. Treasure T. Elective replacement of the aortic root in Marfan's syndrome. Br Heart J 1993; 69:101–103.
18. Chien D, Saloner D, Laub G, Anderson CM. High resolution cine MRI of vessel distention. J Comput Assist Tomogr 1994; 18:576–580.
19. Adams JN, Brooks M, Redpath TW, et al. Aortic distensibility measured by magnetic resonance imaging in patients with Marfan's syndrome. Br Heart J 1995; 73: 265–269.
20. Mohiaddin RH, Firmin DN, Longmore DB. Age related changes of human aortic flow wave velocity measured noninvasively by magnetic resonance imaging. J Appl Physiol 1993; 74:492–497.
21. Groenink M, de Roos A, Mulder BJM, Spaan JAE, van der Wall EE. Changes in aortic distensibility and pulse wave velocity assessed with magnetic resonance imaging following beta-blocker therapy in the Marfan syndrome. Am J Cardiol 1998; 82:203–208.
22. De Paepe A, Devereux RB, Dietz HC, Hennekam RCM, Pyeritz RE. Revised diagnostic criteria for the Marfan syndrome. Am J Med Genet 1996; 62:417–426.
23. Du Bois D, Du Bois EF. A formula to estimate the approximate surface area if height and weight be known. Arch Int Med 1916; 17:863–872.
24. Nichols WW, O'Rourke MF. McDonald's blood flow in arteries: theoretical, experimental and clinical principles. 4th ed. London, England: Arnold, 1998; 57.
25. Lehmann ED. Biophysical properties of the aorta. Lancet 1994; 344:1763.
26. Jeremy RW, Huang H, Hwa J, McCarron H, Hughes CF, Richards JG. Relation between age, arterial distensibility and aortic dilatation in the Marfan syndrome. Am J Cardiol 1994; 74:369–373.
27. Schlatmann TSJM, Becker AE. Pathogenesis of dissecting aneurysm of aorta: comparative histopathologic study of significance of medial changes. Am J Cardiol 1977; 39:21–26.
28. Yin FCP, Brin KP, Ting CT, Pyeritz RE. Arterial hemodynamic indexes in Marfan's syndrome. Circulation 1989; 79:854–862.
29. Hirata K, Triposkiadis F, Sparks E, Bowen J, Wooley CF, Boudoulas H. The Marfan syndrome: abnormal elastic properties. J Am Coll Cardiol 1991; 18:57–63.
30. Savolainen A, Keto P, Hekali P, et al. Aortic distensibility in children with the Marfan syndrome Am J Cardiol 1991; 70: 691–693.
31. Sonesson B, Hansen F, Länne T. Abnormal mechanical properties of the aorta in Marfan's syndrome. Eur J Vasc Surg 1994; 8:595–601.
32. Franke A, Mühler EG, Klues HG, et al. Detection of abnormal elastic properties in asymptomatic patients with Marfan syndrome by combined transoesophageal echocardiography and acoustic quantification. Heart 1996; 75:307–311.
33. Latham RD, Westerhof N, Sipkema P, Rubal BJ, Reuderink P, Murgo JP. Regional wave travel and reflections along the human aorta: a study with six simultaneous micromanometric pressures. Circulation 1985; 72:1257–1269.
34. Luchsinger PC, Snell RE, Patel DJ. Instantaneous pressure distribution along the human aorta. Circ Res 1964; 15:503–510.
35. Fontenier G, Merillon JP, Lerallut JF, Jaffrin MY, Motte G. Aortic pressure and velocity signals processing: application to human aorta characterization. J Physiol (Paris) 1980; 76:741–747. [French]
36. Hardy CJ, Bolster BD, McVeigh ER, Adams WJ, Zerhouni EA. A one-dimensional velocity technique for NMR measurement of aortic distensibility. Magn Reson Med 1994; 31:513–520.
37. Hardy CJ, Bolster BD, McVeigh ER, Iben IET, Zerhouni EA. Pencil excitation with interleaved Fourier velocity encoding: NMR measurement of aortic distensibility. Magn Reson Med 1996; 35:814–819.